International Journal of Heat and Mass Transfer 56 (2013) 206–211

Contents lists available at SciVerse ScienceDirect

International Journal of Heat and Mass Transfer

journal homepage: www.elsevier.com/locate/ijhmt

A unit cell approach to compute thermal conductivity of uncured silicone/phosphor composites

Chao Yuan, Xiaobing Luo *

School of Energy and Power Engineering, Huazhong University of Science and Technology, Wuhan 430074, China

ARTICLE INFO

Article history:
Received 16 June 2012
Received in revised form 8 September 2012
Accepted 21 September 2012

Keywords:
Silicone/phosphor composites
Thermal conductivity
Volume fraction
Interface resistance
Percolation

ABSTRACT

Composites of silicone matrix filled with phosphor are widely used in light emitting diodes (LEDs) packaging. Its thermal conductivity is one of the important properties for LED thermal analysis. In this paper, a unit cell model (UCM) that includes interface resistance between phosphor and silicone matrix was built and applied to predict the thermal conductivity of uncured silicone/phosphor composites at different phosphor volume fractions. The thermal conductivities of seven uncured silicone/phosphor composites samples were measured for comparison with modeling results. The comparison shows that the model result matches to the experimental data within ±6% at the low volume fraction from 3.8% to 25%. Both the experiment and modeling results show that thermal conductivity of the composite has a sudden increase when volume fraction increases to near 40%, which can be explained by the percolation theory. For higher volume fraction, the effect of the interface resistance R_b between the phosphor fillers and silicone matrix cannot be neglected.

1. Introduction

In recent years, lighting emitting diodes (LEDs) have attracted considerable interest due to their high efficiency, good reliability, long lifetime, diverse color and low power consumption. They have begun to play a significant role in many applications [1]. Composites of silicone matrix filled with phosphor, as a light converting layer, are widely used in LED packaging. They are coated on LED chip, when LED chip generates light and heat, part of the heat transfers to the phosphor silicone layer, and then to the ambient. The generated light also passes through the phosphor silicon layer and part of them convert into heat. So, thermal conductivity of silicone/phosphor composites has great influence on heat dissipation of LED chip, which directly determine the reliability and lifetime of the LED. Studying the thermal conductivity of the composite is very important to the research and application of LED packaging. So far, it has not been well analyzed in the literatures even people are highly concerned on it. It is valuable to find an approach to determine the thermal conductivity of this composite.

Past literatures abound with theoretical analysis of thermal conductivity of structure composites. The Maxwell–Garnett (MG) effective medium model [2] matches data for low filler volume fraction. For high volume fraction, Bruggeman's symmetric model (BSM) [3] can be used to predict the electrical conductivity of composites. However, it could not be considered a good model for predicting the thermal conductivity. One of the biggest drawbacks of BSM is that it does not contain the interface resistance R_b which exactly exists between the particle and the matrix [4]. Thermal interface resistance is caused by the imperfect mixing of the particle with the matrix, or due to the phonon acoustic mismatch, or a combination of both [5]. Every et al. [6] established a modified Burggeman model, which is known as the Bruggeman's asymmetric model (BAM). This model has the ability to predict the thermal conductivity for high filler concentrations and it contains the effect of R_b.

Apart from the theoretical models mentioned above, thermal conductivity of composites can also be computed by numerical methods. Kim and Torquato [7,8] studied the effective thermal conductivity of particulate suspensions in regular and random distributions by Brownian motion simulation. This method was demonstrated to accurately predict the effective thermal conductivity with a comparatively fast execution time. Kanuparthi et al. [9] applied a hierarchical meshless computational procedure to simulate the heat transfer in microstructures. This method has the ability to analyze alternative configuration without remeshing. Tang et al. [10,11] developed the uni-directional tow model to predict the degradation in transverse thermal conductivity of laminate or woven composites with complex geometries. They found that the degradation of the conductivity was due to wake debonded cracks for both the DLR-XT plain weave and HITCO 8-Hardness Strain weave. Numerical techniques such as percolation models [12–15] and the finite differences method [16] have also proven to be powerful to compute the thermal conductivity of the composites.

* Corresponding author. Tel.: +86 13971460283; fax: +86 27 87557074.
E-mail address: Luoxb@mail.hust.edu.cn (X. Luo).

0017-9310/$ - see front matter © 2012 Elsevier Ltd. All rights reserved.
http://dx.doi.org/10.1016/j.ijheatmasstransfer.2012.09.053

Nomenclature

Bi	Biot number
h	heat transfer coefficients, W m^{-2} K^{-1}
H	composite thickness, m
k_{eff}	effective composite thermal conductivity, W m^{-1} K^{-1}
k_f	filler thermal conductivity, W m^{-1} K^{-1}
k_m	matrix thermal conductivity, W m^{-1} K^{-1}
k_{mean}	mean composite thermal conductivity, W m^{-1} K^{-1}
l	element dimension (diameter of filler), m
l_c	critical particle diameter, m
L	composite width, m
m	number of elements in the thickness direction
n	number of elements in the width direction
n_t	total numbers of filler elements
Q	total heat flow through the composite, W
R	thermal resistance, m K W^{-1}
R_b	thermal interface resistance, m^2 K W^{-1}
R_{tot}	total thermal resistance of the composite, m K W^{-1}
T	temperature, K
V_p	volumes of phosphor fillers, m^3
V_s	volumes of silicone matrix, m^3

Greek

φ	filler volume fraction

Subscripts

1	upper surface of the composite
2	lower surface of the composite
i, j	indices for mesh

As to percolation models, they are strictly valid only near the percolation threshold and when the ratio of the conductivity of filler and matrix, k_f/k_m, is infinite [4], however, to some composites, like the silicone/phosphor composites, the volume fraction of the filler is normally not as high as the percolation threshold and k_f/k_m is not large enough to meet the precondition of the percolation models. The finite differences method by using a unit cell approach [16] has been built only for theoretical research. The unit cell contains typical properties of particles and matrix material, so the whole elements can represent the actual composite well. Furthermore, the method has much less number of elements than that in other finite element modelings. Also in this approach, the value of k_f/k_m does not have any effect on the prediction of the thermal conductivity.

In the past, few people have attempted to study the thermal conductivity of silicone/phosphor composites. In our former work [17], we measured the thermal conductivity of the cured silicone/phosphor composites for different phosphor volume fractions at different temperatures and also did the numerical simulation in which the diameters of the phosphor were generated by the Monte Carlo method. We found that the results by simulation and experiment matched well. However, we still did not find an appropriate approach to predict the thermal conductivity of the silicone/phosphor composites precisely and readily. Also, in the experiment and simulation [17], the maximum phosphor volume fraction was only 30%.

In this paper, a unit cell model was built and applied to predict the thermal conductivity of uncured silicone/phosphor composites. This model includes the effect of thermal interface resistance R_b and is not dependent on the value of k_f/k_m. The comparisons between experimental and modeling results indicate this model predicts the thermal conductivity of silicone/phosphor composites well at a certain volume fraction. Percolation phenomenon and interface resistance between the phosphor fillers and silicone matrix are also analyzed.

2. Unit cell model

2.1. Geometry in the model

According to the typical geometry of silicone/phosphor composite in high power LED packaging, a two-dimensional model is employed and shown in Fig. 1. All elements' shape of the compound is treated as square for simplicity. The white squares represent the matrix elements with the thermal conductivity k_m, while the filler elements with thermal conductivity k_f are presented by the shaded squares. The dimension of each square is $l \times l$ and l is equal to the diameter of the filler. The thickness H is equal to the number of elements in the thickness direction multiplied by l, which is expressed as $m \times l$. The width L is equal to the number of elements in the width direction multiplied by l, which is expressed as $n \times l$.

2.2. Boundary conditions

The composite is configured to lie between a heat source at temperature T_1 (upper surface) and a heat sink at temperature T_2 (lower surface). The heat transfer coefficients at upper and lower surfaces are h_1 and h_2. The right and left sides of the composite are regarded to be insulated. Generally, a thermal interface resistance R_b exists between the filler elements and any of their neighboring elements.

2.3. Thermal resistance network

Fig. 2 shows a section of the network near the lower left-hand corner of the composite. Each node represents the temperature of one element in Fig. 1. The thermal resistances surrounding the i, j node are marked in Fig. 2, where $R_{ij,U}$ is the upper resistance, $R_{ij,R}$ is the right resistance, $R_{ij,B}$ is the bottom resistance, and $R_{ij,L}$ is the left resistance. These resistances are determined by the two adjacent nodal elements. For the i, j node, these resistances are given by

$$R_{ij,U} = R_{i,j} + R_{i-1,j} \tag{1}$$

$$R_{ij,L} = R_{i,j} + R_{i,j-1} \tag{2}$$

$$R_{ij,B} = R_{i,j} + R_{i+1,j} \tag{3}$$

$$R_{ij,R} = R_{i,j} + R_{i,j+1} \tag{4}$$

In Fig. 2, the i, j node is a matrix element, and the i, $j+1$ node is a filler element. There are following expressions.

$$R_{i,j} = \frac{1}{2k_{i,j}} \tag{5}$$

and

$$R_{i,j+1} = \frac{R_b}{l} + \frac{1}{2k_{i,j+1}} \tag{6}$$

where there are $k_{i,j} = k_m$ and $k_{i,j+1} = k_f$. We notice that the interface resistance R_b will appear when there is a filler element. The other

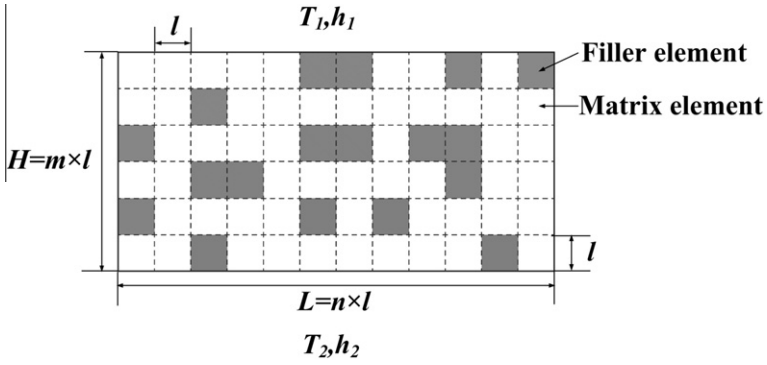

Fig. 1. Thermal model of two-dimensional composite material. T_1 and T_2 are uniform surface temperatures, and h_1 and h_2 are heat transfer coefficients.

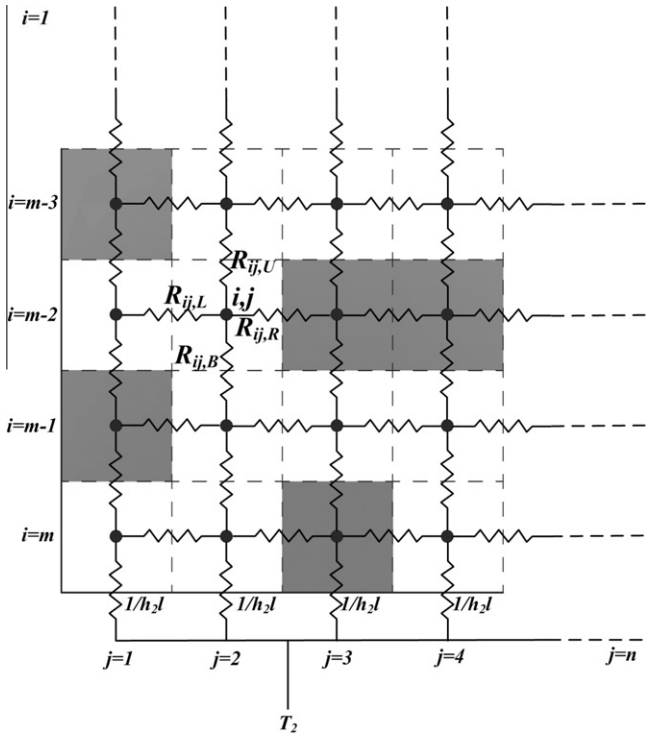

Fig. 2. Lower left-hand section of thermal resistance network.

resistances around the i, j node can be determined by the completely analogous way, and thus all the resistances in the network can be determined except for the top ($i = 1$) and bottom ($i = m$) rows of the network, where the resistances are determined by the heat transfer coefficients shown in Fig. 2.

Based on Kirchhoff Current Law (KCL) [18], the algebraic sum of all the heat flows of each node is zero. For example, for the i, j node in the matrix shown in Fig. 2, we have

$$\frac{T_{i-1,j}-T_{i,j}}{R_{ij,U}}+\frac{T_{i,j+1}-T_{i,j}}{R_{ij,R}}+\frac{T_{i+1,j}-T_{i,j}}{R_{ij,B}}+\frac{T_{i,j-1}-T_{i,j}}{R_{ij,L}}=0 \tag{7}$$

Such an equation can be written for each node. All the equations can form a matrix equation $BT = C$, where B is an $(m \times n) \times (m \times n)$ coefficient matrix, C is a vector of length $m \times n$, and T is a vector of length $m \times n$, it contains the nodal temperature needed to be solved.

2.4. Determining the positions of the filler elements

The total numbers of filler elements n_t is equal to the filler volume fraction φ multiplied by the total numbers of nodes, which is expressed as $\varphi \times (m \times n)$. Here we use the random number generator to determine which nodes are occupied by the filler.

2.5. Determining the thermal conductivity of the composite

After obtaining the temperature at each node, the total heat flow Q through the composite can be determined by summing up all the individual nodal heat flows at either the upper or lower composite boundary [16]. Then, the total thermal resistance of the composite can be calculated

$$R_{tot}=\frac{T_1-T_2}{Q} \tag{8}$$

We can also have another expression for the total thermal resistance between T_1 and T_2,

$$R_{tot}=\frac{1}{h_1 L}+\frac{H}{k_{eff}L}+\frac{1}{h_2 L} \tag{9}$$

Then the effective thermal conductivity of composite k_{eff} is determined by

$$k_{eff}=\frac{H}{L\left(\frac{T_1-T_2}{Q}\right)-\frac{1}{h_1}-\frac{1}{h_2}} \tag{10}$$

We found that the average results of 300 iterations had just 0.3% deviation with the values of 1000 iterations. In order to get an average value k_{mean} of k_{eff}, a total of 300 iterations were performed to determine an acceptable value. Usually, the mean size of phosphor particles in LED packaging is 13 μm in diameter, thus l is fixed at 13 μm. The thermal conductivities of the uncured silicone k_m and the phosphor k_f are 0.16 W m^{-1} K^{-1} and 13 W m^{-1} K^{-1}. All calculations are performed for $R_b = 0$ m^2 K W^{-1}, $T_1 = 300$ K, and $T_2 = 290$ K. It should be noted that the composite thermal conductivity has no connection to the differential of the boundary temperatures in UCM. A matrix width and thickness are 20 and 40 times of the particle diameter, respectively, meaning that $m = 20$ and $n = 40$. This was done because a matrix with this size adequately represents a bulk material. Fig. 3 presents the effect of thickness on the thermal conductivity for different volume fractions φ when any effect of interface resistance is neglected by taking $R_b = 0$ m^2 K W^{-1}. As shown in Fig. 3, at large thicknesses, the curves are close to horizontal lines. This indicates that k_{mean} becomes independent of thickness at some points. With that size, the matrix can adequately stand for a bulk material. Based on the

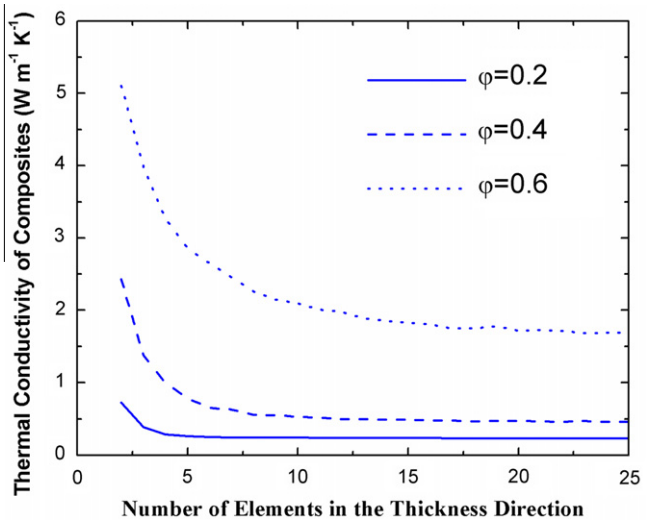

Fig. 3. Effect of thickness on thermal conductivity at a constant width k_f = 13 - W m^{-1} K^{-1}, k_m = 0.16 W m^{-1} K^{-1}, R_b = 0 m^2 K W^{-1}).

above discussion, the number of elements in the thickness direction, m, is chosen to be 20 to guarantee the computation accuracy and save the calculation time.

3. Experiments

The silicone/phosphor composites are prepared by mixing uncured silicone with phosphor powders at different volumetric concentrations. The phosphor volume fraction, φ, is defined as follows: [19]

$$\varphi = \frac{V_p}{V_p + V_s} \tag{11}$$

where V_p and V_s are the volumes of phosphor fillers and silicone matrix respectively. To aid in the wetting of the fillers and prevent the re-agglomeration of the fillers, the phosphor powders are surface treated. And then, in order to remove air bubbles, the mixture is placed in a vacuum chamber until no bubbles emerge.

In the experiments, the thermal conductivities of uncured silicone/phosphor composites are measured at 15 °C by transient hot-wire method. A schematic diagram of the test sensor is shown in Fig. 4. The hot wire with extremely tiny diameter is coated by Teflon. For the measurement of uncured silicone/phosphor composites, a beaker was used to contain the samples which the sensor was put into. After heating the hot wire, the samples have temperature rise in a defined distance from the heat source. By measuring the temperature change over a known time interval, the thermal conductivity can be derived from the one-dimensional transient heat conduction equation.

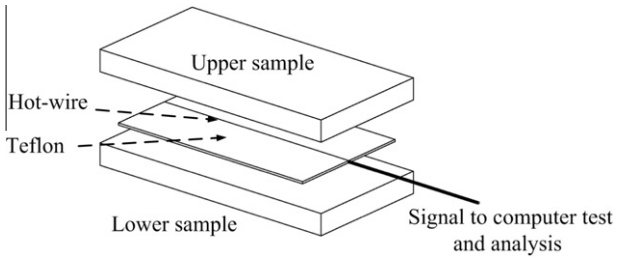

Fig. 4. Schematic of transient hot-wire sensor.

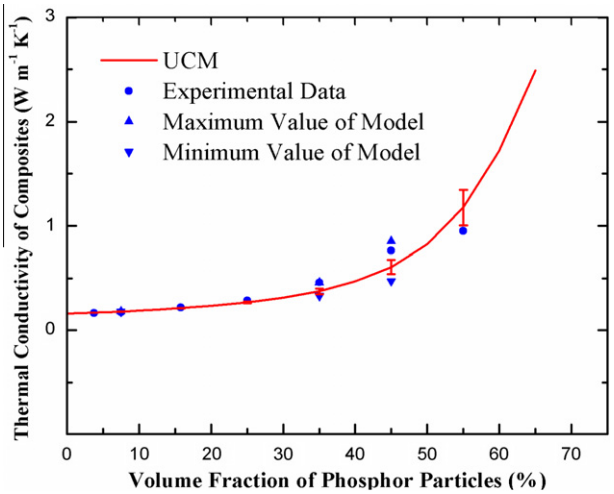

Fig. 5. Comparison of modeling result with experimental data for R_b = 0 m^2 K W^{-1}.

Table 1
Deviation analysis between modeling and experimental data at different volume fraction.

Volume fraction of phosphor (%)	Model prediction data (W m^{-1} K^{-1})	Experimental data (W m^{-1} K^{-1})	Deviation (%)
3.8	0.1697	0.1680	−1.00
7.5	0.1810	0.1750	−3.31
15.8	0.2128	0.2200	3.38
25.0	0.2690	0.2850	5.95

In the experiments, all the samples were measured for five times and the mean value of them were calculated.

4. Comparison and analysis

Fig. 5 shows the comparison between the present model's prediction and experimental results at different phosphor volume fractions. 0% volume fraction represents pure silicone. It is found that the UCM predictions match to the experimental data within ±6% at the low volume fraction from 3.8% to 25%. The details of the error analysis from 3.8% to 25% are given in Table 1. Considering that the volume fraction is normally lower than 20% in usual LED packaging, UCM can provide good prediction for the thermal conductivity of packaging materials in real applications.

Fig. 5 also indicates that at constant temperature, the higher the volume fraction of phosphor is, the higher is the thermal conductivity. Until 35% volume fraction, the increase of thermal conductivity becomes slight. However, there is a sudden increase in thermal conductivity when volume fraction increases to near 40%, which can be explained by the percolation theory.

Fig. 6 shows a case when percolation has taken place at a certain percentage of phosphor particles, called percolation threshold. The phosphor particles form a continuous chain from one surface to another and make the thermal energy pass through the region more easily than others, as a result, the conductivity of silicone/phosphor composites increase rapidly [15].

Fig. 5 also shows that the experimental results at 35% and 45% volume fractions are slightly larger than the model predictions. Actually, when the volume fraction increases to near the percolation threshold, there is the possibility for the phosphor particles to form the continuous path as shown in Fig. 6 to make the conductivity high. In the experiment, at the percolation threshold, the

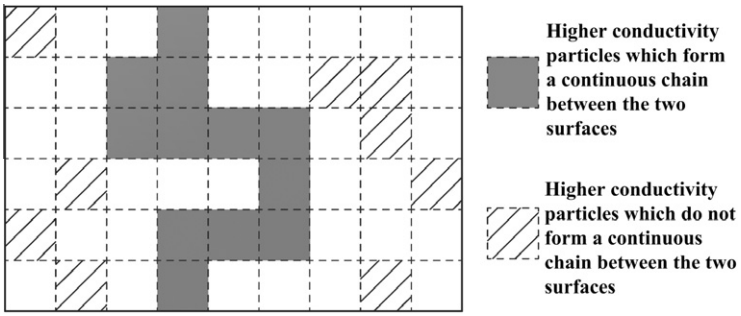

Fig. 6. Percolation phenomenon occurring when a continuous chain is formed between the two surfaces by particles with high thermal conductivity.

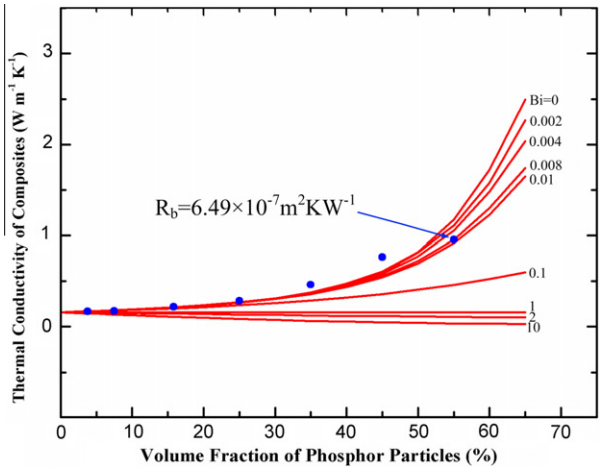

Fig. 7. Estimation of R_b by present model.

phosphor particles in the composites are inclined to cluster [17], the test equipment can catch this. But in the modeling, because of the probabilistic nature of this approach, the differential of thermal conductivities in different calculations at the same volume fraction could be large. For example, at the 45% volume fraction, the differential between the maximum and minimum thermal conductivity in the model calculation is 0.3773 W m^{-1} K^{-1}, but k_{mean} at 45% volume fraction is 0.6148 W m^{-1} K^{-1}. So in the modeling, to get an acceptable average value, we operated the model 300 times for each volume fraction. Based on the above discussion, we can see that the experiment can catch the particle cluster phenomena, but the modeling uses the averaging calculation data, so at the percolation threshold, the experimental results for thermal conductivity is slightly higher than that by the present model.

Fig. 5 also illustrates the overprediction of the thermal conductivity at 55% volume fraction when neglecting the interface resistance R_b between the phosphor particles and the silicone matrix. When discussing R_b, the dimensionless variable called the Biot number Bi is often used, which is defined as [20]

$$Bi = \frac{R_b k_m}{l} \tag{12}$$

where k_m is the thermal conductivity of the base matrix, l is the particle diameter, R_b is the thermal interface resistance. It can be seen that Bi is directly proportional to R_b.The critical particle diameter l_c is defined by setting $Bi = 1$ [20]:

$$l_c = R_b k_m \tag{13}$$

In order to estimate the R_b at 55% volume fraction, we take a variety of Bi numbers to plot the curves under different R_b by using the UCM.

Fig. 7 shows the dependence of thermal conductivities on volume fraction under different Bi numbers. It is found that the prediction data under $Bi = 0.008$ and $R_b = 6.49 \times 10^{-7}$ m^2 K W^{-1} fits well with the experimental data at 55% volume fraction. In Fig. 7, we can see that the interface resistance has little effect on the thermal conductivity of this composite when the volume fraction is very low. As the volume fraction is larger than 0.1, the thermal conductivity decreases under the same volume fraction as R_b increases.

According to Eq. (13), when Bi number is equal to 1, the phosphor particles diameter l is the same as the critical particle diameter l_c. For this case, the thermal conductivity of the composite is nearly the same as that of silicone matrix. And if the phosphor particles diameter l is smaller than the critical particle diameter l_c, the thermal conductivity of silicone/phosphor composites is lower than that of silicone matrix even the phosphor has a higher thermal conductivity than that of silicone. Based on the above facts, it can be seen that the critical particle diameter is an important parameter to decide the thermal conductivity of composites.

5. Conclusions

A UCM model for predicting the thermal conductivity of uncured silicone/phosphor composites was proposed in this paper. Experiments were conducted to prove this model. The comparison proves that the UCM predicts well at the low phosphor fraction below 25%. The comparison also shows that the effect of the thermal interface resistance between the fillers and matrix cannot be neglected at high filler volume fraction. The present model is also able to reflect the percolation phenomenon and estimate the percolation threshold of the silicone/phosphor composites.

Acknowledegments

The authors would like to acknowledge the financial support in part from 973 Project of The Ministry of Science and Technology of China (2009CB320203, 2011CB013105), and in part by National 863 project of The Ministry of Science and Technology of China (2011AA03A109).

References

[1] S. Liu, X.B. Luo, LED Packaging for Lighting Applications: Design, Manufacturing, and Testing, John Wiley & Sons Press, USA, 2011.
[2] D.P.H. Hassleman, L.F. Johnson, Effective thermal conductivity of composites with interfacial thermal barrier resistance, J. Compos. Mater. 21 (6) (1987) 508–515.
[3] R. Landauer, Electrical conductivity in inhomogeneous media, AIP Conf. Proc. 40 (1) (1978) 2–45.
[4] R.S. Prasher, Thermal interface materials: historical perspective, status, and future directions, Proc. IEEE 94 (8) (2006) 1571–1586.
[5] R.S. Prasher, O. Alger, P.E. Phelan, A unified macroscopic and microscopic approach to contact conduction heat transfer, in: Proceedings of 35th National Heat Transfer Conference, Anaheim, CA, 2001.

[6] A.G. Every, Y. Tzou, D.P.H. Hassleman, R. Raj, The effect of particle size on the thermal conductivity of ZnS/diamond composites, Acta Metall. Mater. 40 (1) (1992) 123–129.
[7] C. Kim, S. Torquato, Determination of the effective thermal conductivity of heterogeneous media by Brownian motion simulation, J. Appl. Phys. 68 (8) (1990) 3892–3903.
[8] C. Kim, S. Torquato, Effective conductivity of suspensions of hard spheres by Brownian motion simulation, J. Appl. Phys. 69 (4) (1991) 2280–2289.
[9] S. Kanuparthi, M. Rayasam, G. Subbarayan, B. Sammakia, A. Gowda, S. Tonapi, Hierarchical field compositions for simulations of near-percolation thermal transport in particulate materials, Comput. Methods Appl. Mech. Eng. 198 (5–8) (2009) 657–668.
[10] C. Tang, M. Blacklock, D.R. Hayhurst, Uni-axial stress–strain response and thermal conductivity degradation of ceramic matrix composite fibre tows, Proc. R. Soc. A-Math. Phys. Eng. Sci. 465 (2009) 2849–2876.
[11] C. Tang, M. Blacklock, D.R. Hayhurst, Stress–strain response and thermal conductivity degradation of ceramic matrix composite fibre tows in 0°–90° uni-directional and woven composites, J. Compos. Mater. 45 (14) (2011) 1461–1482.
[12] A.E. Morozovskii, A.A. Snarskii, Finite scaling of the effective conductivity in percolation systems with nonzero ratio of the phase conductivities, JETP 82 (2) (1996) 361–365.
[13] X.G. Liang, J.R. Lukes, C.L. Tien, Anisotropic thermal conductance in thin layers of disordered packed spheres, in: 11th International Heat Transfer Conference, vol. 7, 1998, pp. 33–38.
[14] X.G. Liang, X. Ji, Thermal conductance of randomly oriented composites of thin layers, Int. J. Heat Mass Transfer 43 (19) (2000) 3633–3640.
[15] A. Devpura, P.E. Phelan, R.S. Prasher, Percolation theory applied to the analysis of thermal interface materials in flip-chip technology, Therm. Thermomech. Phenom. Electron. Syst. 1 (2000) 21–28.
[16] P.E. Phelan, R.C. Niemann, Effective thermal conductivity of a thin, randomly oriented composite material, J. Heat Transfer 120 (4) (1998) 971–977.
[17] Q. Zhang, Z.H. Pi, M.X. Chen, X.B. Luo, L. Xu, S. Liu, Effective thermal conductivity of silicone/phosphor composites, J. Compos. Mater. 45 (23) (2011) 2465–2474.
[18] A. Charles, S. Matthew, Fundamentals of Electric Circuits 3, McGraw-Hill, 2006. pp. 37–43.
[19] K. Sanada, Y. Tada, Y. Shindo, Thermal conductivity of polymer composites with close-packed structure of nano and micro fillers, Compos. Part A: Appl. Sci. Manufact. 40 (6–7) (2009) 724–730.
[20] A. Devpura, P.E. Phelan, R.S. Prasher, Size effects on the thermal conductivity of polymers laden with highly conductive filler particles, Microscale Thermophys. Eng. 5 (2001) 177–189.